Reconciling Simulated Moisture Fluxes Resulting from Alternate Hydrologic Model Time Steps and Energy Budget Closure Assumptions

INGJERD HADDELAND

Department of Geosciences, University of Oslo, and Norwegian Water Resources and Energy Directorate, Oslo, Norway

DENNIS P. LETTENMAIER

Department of Civil and Environmental Engineering, University of Washington, Seattle, Washington

THOMAS SKAUGEN

Department of Geosciences, University of Oslo, and Norwegian Water Resources and Energy Directorate, Oslo, Norway

(Manuscript received 25 February 2005, in final form 10 August 2005)

ABSTRACT

Hydrological model predictions are sensitive to model forcings, input parameters, and the parameterizations of physical processes. Analyses performed for the Variable Infiltration Capacity model show that the resulting moisture fluxes are sensitive to the time step and energy balance closure assumptions. In addition, the model results are sensitive to the method of spatial and temporal disaggregation of precipitation. For parameter estimation purposes, it is desirable to do parameter searches in water balance mode (meaning that the effective surface temperature is assumed equal to the surface air temperature; hence no iteration for energy balance closure is performed) at daily time steps. However, transferring these parameters directly to other model modes (e.g., energy balance, in which an iteration for effective surface temperature is performed, and/or different model time steps) results in changes in the simulated moisture fluxes. The simulated differences in moisture fluxes are mainly a result of the parameterization of evapotranspiration at different time steps and model modes. A simple scheme that calculates correction factors for some model parameters is developed. The scheme is used to match simulated moisture fluxes in hourly and 3-hourly energy balance mode to the daily water balance simulation results, and to match hourly energy balance runs using spatially and temporally disaggregated precipitation to 3-hourly energy balance runs using uniformly disaggregated precipitation. For both approaches, the corrected simulations match the baseline simulations quite closely, both over transects across much of the continental United States and for test applications in the Ohio and Arkansas–Red River basins.

1. Introduction

In hydrological modeling, the time step used often depends on the purpose of the model simulations. For flood forecasting, hourly time steps might be needed, while daily, or even longer, time steps may be sufficient for water supply forecasts and reservoir modeling. Land surface schemes coupled to atmospheric models are often run at time steps of only a few minutes, a time resolution for which validation data (e.g., streamflow observations) rarely exist. In addition, some physically based hydrologic models and land surface schemes used for offline hydrologic modeling have the option of solving the surface energy balance (i.e., iterating for energy balance closure by solving for one or more effective surface temperatures). We term this "energy balance mode," in contrast to "water balance mode," in which the surface temperature is assumed equal to the surface air temperature, and no iteration is performed. Essentially all operational hydrology models operate in this latter (water balance) mode.

Accurate and effective estimation of model parameters is critical in hydrological modeling. Although field observations can be utilized in parameter estimation for hydrologic models, calibration has been shown to im-

Corresponding author address: Ingjerd Haddeland, Dept. of Geosciences, University of Oslo, Box 1022, Blindern, NO-0315 Oslo, Norway.
E-mail: ingjerd.haddeland@geo.uio.no

© 2006 American Meteorological Society

Unauthenticated | Downloaded 04/30/21 12:30 PM UTC

prove the results even for physically based models (Wood et al. 1998; Nijssen et al. 2003). Hydrologic model experiments have shown substantial sensitivity to the spatial and temporal resolution at which the model is run (Boone et al. 2004; Vérant et al. 2004; Haddeland et al. 2002; Schaake et al. 1996), and simulated streamflow, in particular, has been shown to be dependent on the temporal resolution of precipitation (Holman-Dodds et al. 1999). Lohmann et al. (2004) demonstrated that for the Variable Infiltration Capacity (VIC) model, the model time step used, and the method of temporal and spatial disaggregation of precipitation, can have large effects on simulated streamflow.

As noted above, most operational hydrologic models operate in water balance mode, while some research models, and most land surface schemes, operate in energy balance mode. The water versus energy balance issue, and its effect on model simulations, has not received much attention. The VIC macroscale hydrology model (Liang et al. 1994) can be run in two modes: energy or water balance. The water balance mode is much more computationally efficient than the energy balance mode, but the energy balance mode more closely reflects the use of the model in fully coupled land–atmosphere applications. For parameter estimation purposes, it is desirable to perform parameter searches in water balance mode, but understanding the implications of model performance for a given set of parameters in energy balance mode is clearly important. Furthermore, the energy balance mode often requires shorter time steps to avoid numerical and conceptual problems.

The objective of this paper is to explain how the choice of time step and energy balance closure assumptions influences resulting moisture fluxes in the VIC model, and subsequently to develop a method that can be used to reproduce daily water balance results at other modes and temporal resolutions. Many hydrologic models can be run at a range of model time steps, and the model setups analyzed in this study are representative for operational hydrologic models (daily water balance) and for land surface schemes (subdaily energy balance). The issues studied are general to the hydrologic modeling community, as is the method chosen to reconcile the simulated moisture fluxes. The benefit of establishing a relationship between the modes and temporal resolutions is that the model then can be calibrated in daily water balance mode even if the model will be run at subdaily time steps in energy balance mode. Hence, the calibration computational time can be lowered substantially.

2. Approach

The VIC macroscale hydrologic model (Liang et al. 1994) solves the water and energy balance equations at the land surface. Land cover variability is represented through partitioning each grid cell into multiple vegetation types and bare soil, and the soil column is divided into three soil layers. The saturation excess mechanism, which produces surface runoff, is parameterized through the Xinanjiang variable infiltration curve (Zhao et al. 1980; Wood et al. 1992). Release of base flow from the lowest soil layer is controlled through a nonlinear recession curve. Surface runoff and base flow for each cell can be routed to the basin outlet through a channel network as described by Lohmann et al. (1998).

The VIC model is typically applied at spatial resolutions from ⅛° to 2° latitude by longitude, and at hourly to daily temporal resolutions. In both water and energy balance modes, snow accumulation and ablation processes are solved via an energy balance approach (following Wigmosta et al. 1994) that operates at a subdaily time step, regardless of whether the time step is daily during snow-free periods.

The minimum required input data to the model are daily precipitation and minimum and maximum daily temperatures. When the model is run at subdaily time steps, using daily meteorological forcing data, the model calculates subdaily meteorological data based on the daily input data. Precipitation is averaged over the day, while hourly temperature values are obtained by fitting a spline curve to the daily maximum and minimum temperatures through application of hermite polynomials. When shortwave radiation and vapor pressure are not supplied to the model, these variables are calculated by the model based on daily precipitation and daily minimum and maximum temperatures, using algorithms developed by Thornton and Running (1999) and Kimball et al. (1997) as described by Nijssen et al. (2001). Longwave radiation at each time step is calculated based on Bras (1990, 31–47) and wind speed is assumed constant during the day.

The VIC model has been shown to be capable of reproducing observed streamflow for both water balance and energy balance implementations in various publications (Nijssen et al. 2003; Maurer et al. 2002; Haddeland et al. 2002; among others). The focus of this paper is on differences in moisture fluxes that occur when the model is run at a range of time steps, and for different energy balance closure assumptions. In particular, we introduce an approach that can reconcile these differences by simple parameter adjustments. The

Unauthenticated | Downloaded 04/30/21 12:30 PM UTC

intent of the work is to match the runoff produced at the grid cell level; hence we do not include routing to produce simulated streamflow in this paper.

3. Initial analyses

a. Study areas and model analyses

Four transects in the eastern United States (see Fig. 1) were selected for initial analyses of the differences in model-simulated moisture fluxes associated with various time steps and modes. The transects consist of 340 grid cells of ⅛° (latitude by longitude). The input meteorological forcing data (daily precipitation, minimum and maximum temperatures, and wind speed), and the land-cover data (vegetation and soil parameters), are as reported by Maurer et al. (2002). A single elevation band was used. The differences in resulting moisture fluxes caused by running the model at different time steps and simulation modes were investigated by analyzing daily, 3-hourly, and hourly simulations. For the subdaily time steps, the model was run in both water balance (WB) and energy balance (EB) mode.

Daily precipitation values were distributed uniformly throughout the day when running at subdaily time steps. The baseline analysis is the daily water balance simulations, referred to as 24.WB, while the remaining analyses are referred to as 3.WB, 1.WB, 3.EB, and 1.EB. For each analysis, the model was run for 10 yr (1988–97), after a spinup period of 1 yr. The same model parameters (soil and vegetation characteristics) were used in all simulations.

b. General results

Figure 2 shows mean annual moisture fluxes for each model analysis. The figure shows that, in general, evapotranspiration decreases and total runoff increases when going from 24.WB to 3.WB. The same is observed when going from 3.WB to 3.EB; see also Table 1. The hourly water balance simulations are, however, fairly close to the daily water balance simulations.

Over the 10 yr analyzed, and averaged over all 340 cells in the transects, evapotranspiration at 3.EB and 1.EB is 14% and 7% lower than at 24.WB, and the corresponding increase in total runoff is 27% and 13%, respectively. The runoff ratio increases from 0.34 in 24.WB to 0.43 in 3.EB, whereas the runoff ratio at 1.EB is 0.38. Figure 2 and Table 1 indicate that the drier areas have the relatively largest increases in runoff, and for some cells runoff more than doubles when running the model at 3.EB, compared with the results obtained at 24.WB.

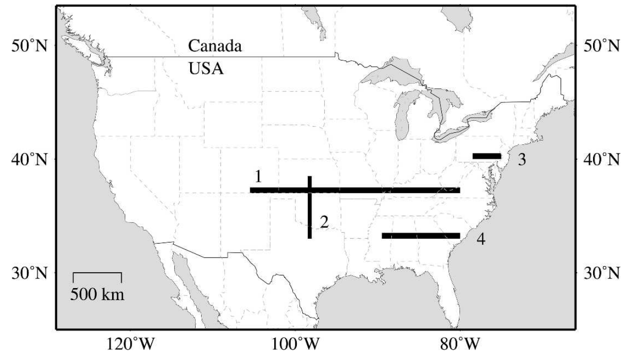

FIG. 1. Location of the four transects used in the initial analyses.

Evapotranspiration in VIC is calculated using a modification of the Penman–Monteith equation (Shuttleworth 1993), which allows net radiation and other heat fluxes to vary throughout the day if so desired. The following sections show that the representation of these variables at subdaily and daily time steps, and the parameterization of canopy interception during the time step in question, will influence resulting evapotranspiration, and hence runoff.

c. Effect of temporal resolution

Over the 10 yr analyzed, evapotranspiration at 3.WB is 9% lower than at 24.WB, and the corresponding increase in total runoff is 17%. The runoff ratio increases from 0.34 in 24.WB to 0.40 in 3.WB. Thus, the difference in time step accounts for 64% of the difference in total runoff between 24.WB and 3.EB. The runoff difference between 24.WB and 1.WB, however, is negligible.

Figure 3 shows that the main reason total evapotranspiration at daily time steps is higher than at 3-hourly time steps is the differences in canopy evaporation (Fig. 3b). The differences can be explained by the scheme used to parameterize canopy evaporation. When VIC is run at daily time steps, canopy evaporation can include the current time step's precipitation. However, when VIC is run at subdaily time steps, canopy evaporation cannot exceed current interception storage. This difference generally favors evaporation of intercepted water at daily time steps. Test simulations demonstrated that if canopy evaporation at daily time steps cannot include current precipitation, evaporation averaged over the transects will be lower at daily time steps than at subdaily time steps (not shown). The higher canopy evaporation values at hourly time steps than at 3-hourly time steps are a result of the assumption of a maximum canopy water holding capacity that does not vary with the time step.

Unauthenticated | Downloaded 04/30/21 12:30 PM UTC

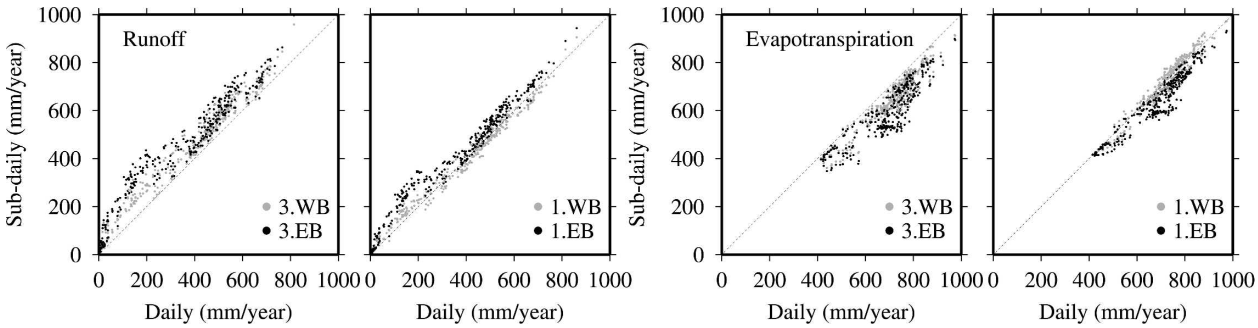

FIG. 2. Mean annual moisture fluxes in each cell in the transects at daily time steps (24.WB), compared to the simulation results at subdaily time steps (3.WB, 3.EB, 1.WB, and 1.EB).

The differences in potential transpiration values (Fig. 3e) indicate that the diurnal variation in forcing data suppresses transpiration, given that soil moisture does not limit transpiration. In VIC, stomatal resistance r_s is dependent on air temperature T, vapor pressure deficit (vpd), shortwave radiation [photosynthetically active radiation (PAR)], and soil moisture availability θ, and is calculated as follows:

$$r_s = \frac{(r_s)_{\min}}{f_1(T)\,f_2(\mathrm{vpd})\,f_3(\mathrm{PAR})\,f_4(\theta)}, \tag{1}$$

where $(r_s)_{\min}$ is minimal stomatal resistance, and the factors in the denominator have values between 0 and 1. The diurnal variation in shortwave radiation, air temperature, and humidity, and hence vapor pressure deficit, results in lower potential transpiration at 3-hourly time steps than at daily time steps (Fig. 3e). However, as a result of the decreased canopy evaporation (Fig. 3b) throughfall increases, and thus available soil moisture at 3-hourly time steps is higher than at daily time steps (Fig. 3d). This results in more or less equal transpiration values at 3.WB and 24.WB (Fig. 3c), despite the reduced transpiration "drive." However, total evapotranspiration at 3-hourly time steps is still lower than at daily time steps (Fig. 3a). The effect of the reduced transpiration drive is clearer when looking at the hourly simulations. Because canopy evaporation is higher at hourly than at 3-hourly time steps (Fig. 3b), soil moisture at hourly and daily time steps is more similar (Fig. 3d), and hence transpiration is lower (Fig. 3c) at hourly time steps than at both 3-hourly and daily time steps. If there were no transpiration limitations (i.e., assuming no canopy resistance), transpiration values at 24.WB, 3.WB, and 1.WB would have been nearly identical (Fig. 3f).

d. Effect of water versus energy balance mode

Simulating the surface fluxes in energy balance mode instead of water balance mode results in an additional decrease in evapotranspiration, and increased runoff. Averaged over the transects, evapotranspiration in energy balance mode is 6% lower than in water balance mode (3-hourly time steps), and total runoff increases by 8%. The corresponding numbers at hourly time steps are 7% and 13%. In energy balance mode, the model iterates at each time step for the surface temperature that results in closure of the surface energy and water budgets. When the VIC model is run in water

TABLE 1. Mean annual moisture fluxes [precipitation (P), evapotranspiration (ET), runoff (Q)] in each transect (mm yr^{-1}).

		Transect number														
		1 (201 cells at 37°N)			2 (41 cells at 98°W)			3 (25 cells at 40°N)			4 (73 cells at 33°N)			All 340 cells		
Analysis	Explanation	P	ET	Q	P	ET	Q	P	ET	Q	P	ET	Q	P	ET	Q
24.WB	Daily water balance	1000	686	315	856	710	143	1103	614	487	1338	756	572	1063	699	362
3.WB	3-hourly water balance	1000	631	371	856	624	231	1103	572	530	1338	683	646	1063	637	424
3.EB	3-hourly energy balance	1000	599	402	856	532	324	1103	563	538	1338	659	669	1063	601	460
1.WB	1-hourly water balance	1000	699	311	856	679	174	1103	623	481	1338	763	565	1063	705	362
1.EB	1-hourly energy balance	1000	649	352	856	599	258	1103	603	499	1338	712	616	1063	653	408

Unauthenticated | Downloaded 04/30/21 12:30 PM UTC

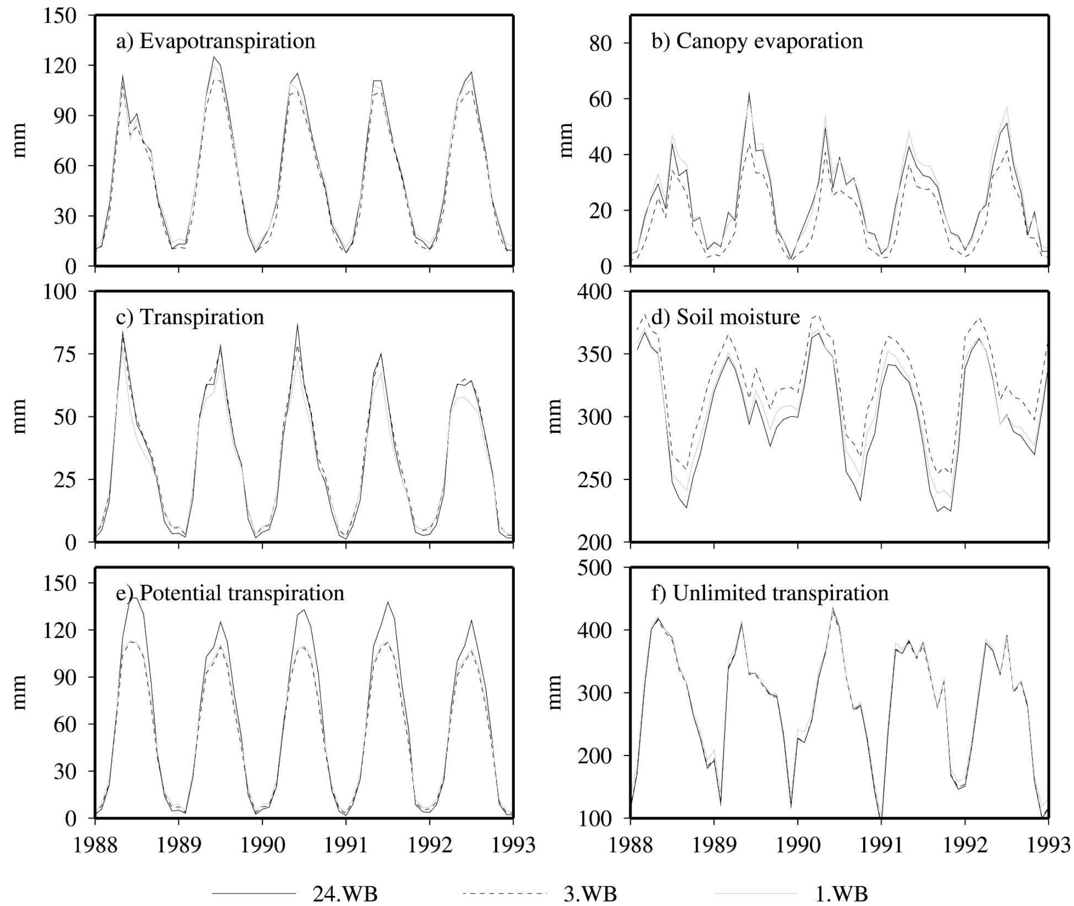

FIG. 3. Monthly values of (a) evapotranspiration, (b) canopy evaporation, (c) transpiration, (d) soil moisture, (e) potential transpiration, and (f) unlimited transpiration for a 5-yr period in transect number 1.

balance mode, the surface energy fluxes are not estimated directly (except when snow is present), and outgoing longwave radiation is calculated based on air temperatures. When comparing the energy balance mode surface temperatures to the water balance air temperatures, it can be seen that the iterated surface temperatures are higher than the air temperatures (Fig. 4a). The difference between surface temperatures in

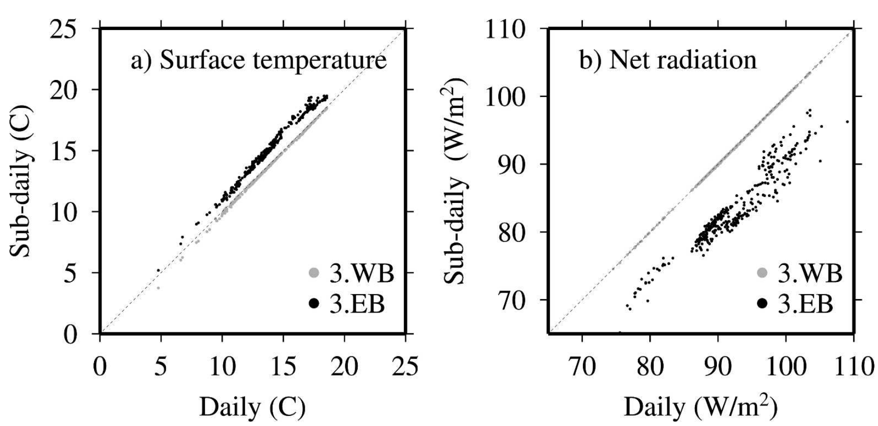

FIG. 4. Mean annual (a) surface temperature and (b) net radiation in each cell in the transects. Daily time steps (24.WB) are compared with subdaily time steps (3.WB and 3.EB).

Unauthenticated | Downloaded 04/30/21 12:30 PM UTC

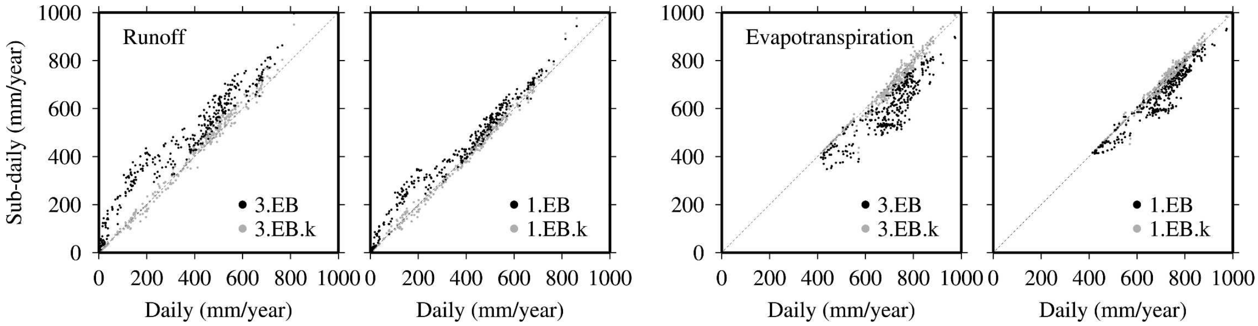

FIG. 5. Mean annual moisture fluxes in each cell in the transects at daily time steps (24.WB) compared with the original and corrected simulation results at 3-hourly time steps (3.EB, 3.EB.k, 1.EB, and 1.EB.k).

energy balance mode and air temperatures in water balance mode is reflected in differences in net radiation in the two modes (Fig. 4b), which indicates increased mean annual outgoing longwave radiation in energy balance mode as compared to water balance mode. One reason evapotranspiration is lower in energy balance mode than in water balance mode is because evapotranspiration is dependent on net radiation.

The effect of atmospheric stability on aerodynamic resistance is calculated using a Richardson approach (Storck 2000, 68–72). Stability corrections are calculated for nonneutral conditions, and thus affect the resulting aerodynamic resistances only when the model is run in energy balance mode (surface temperatures can be different from air temperatures). Aerodynamic resistance impacts potential evapotranspiration, and hence the use of stability correction factors in energy balance mode is another reason simulated evapotranspiration is different in energy balance mode than in water balance mode. The effects on monthly moisture fluxes are small, but evapotranspiration in the wintertime ends up being slightly higher when the use of stability correction factors are excluded from the energy balance simulations.

4. Connecting model modes and temporal resolutions

The previous section has shown that the differences in moisture fluxes seen when evaluating the VIC model at varying temporal scales and using contrasting energy balance closure assumptions are mainly caused by evapotranspiration differences. Assuming that the model is calibrated in daily water balance mode, and that the calibrated simulation results represent true runoff and evapotranspiration values, a scheme that is designed to match subdaily energy balance simulation results to daily water balance simulations is developed. One might argue that the subdaily energy balance runs should have the smallest errors compared to true values, and hence it would be more appropriate to correct the daily water balance runs to the subdaily energy balance runs. The differences seen, especially for canopy evaporation, are mainly results of model parameterizations. Given that the model is calibrated in daily water balance mode, the overall partitioning between runoff and evapotranspiration should therefore be closest to the true values when running the model in that mode. Thorough areal comparisons with field data of evaporation and transpiration would be desirable to evaluate model performance in comparison with observed partitioning between transpiration and evaporation. Data suitable for conducting such analyses across a range of vegetation types are, unfortunately, difficult to come by.

Based on the results from the initial analyses, we decided on the following approach to estimate the parameters that will produce consistent results across temporal scales and modes of model implementation. A search procedure is implemented to determine two correction factors, one for minimal stomatal resistance and architectural resistance R, and one for canopy interception capacity C (liquid precipitation only). For each grid cell, the resistance and interception capacity corrections factors k_1 and k_2, respectively, are the same for all vegetation types within the cell (n: cell, i: vegetation type):

$$(R_{\mathrm{new}})_{n,i} = (R_{\mathrm{orig}})_{n,i} \times k_{1,n} \quad \text{and} \tag{2}$$

$$(C_{\mathrm{new}})_{n,i} = (C_{\mathrm{orig}})_{n,i} \times k_{2,n}. \tag{3}$$

The correction factors were calculated using the Shuffled Complex Evolution Metropolis algorithm (SCE-UA; Vrugt et al. 2003) for every eighth cell in the transects (i.e., one cell per degree latitude or longitude), through the following objective function:

$$\min \sum_{\text{months}} [(\mathrm{EC}_{\mathrm{subdaily}} - \mathrm{EC}_{24.\mathrm{WB}})^2 + (\mathrm{TV}_{\mathrm{subdaily}} - \mathrm{TV}_{24.\mathrm{WB}})^2], \tag{4}$$

Unauthenticated | Downloaded 04/30/21 12:30 PM UTC

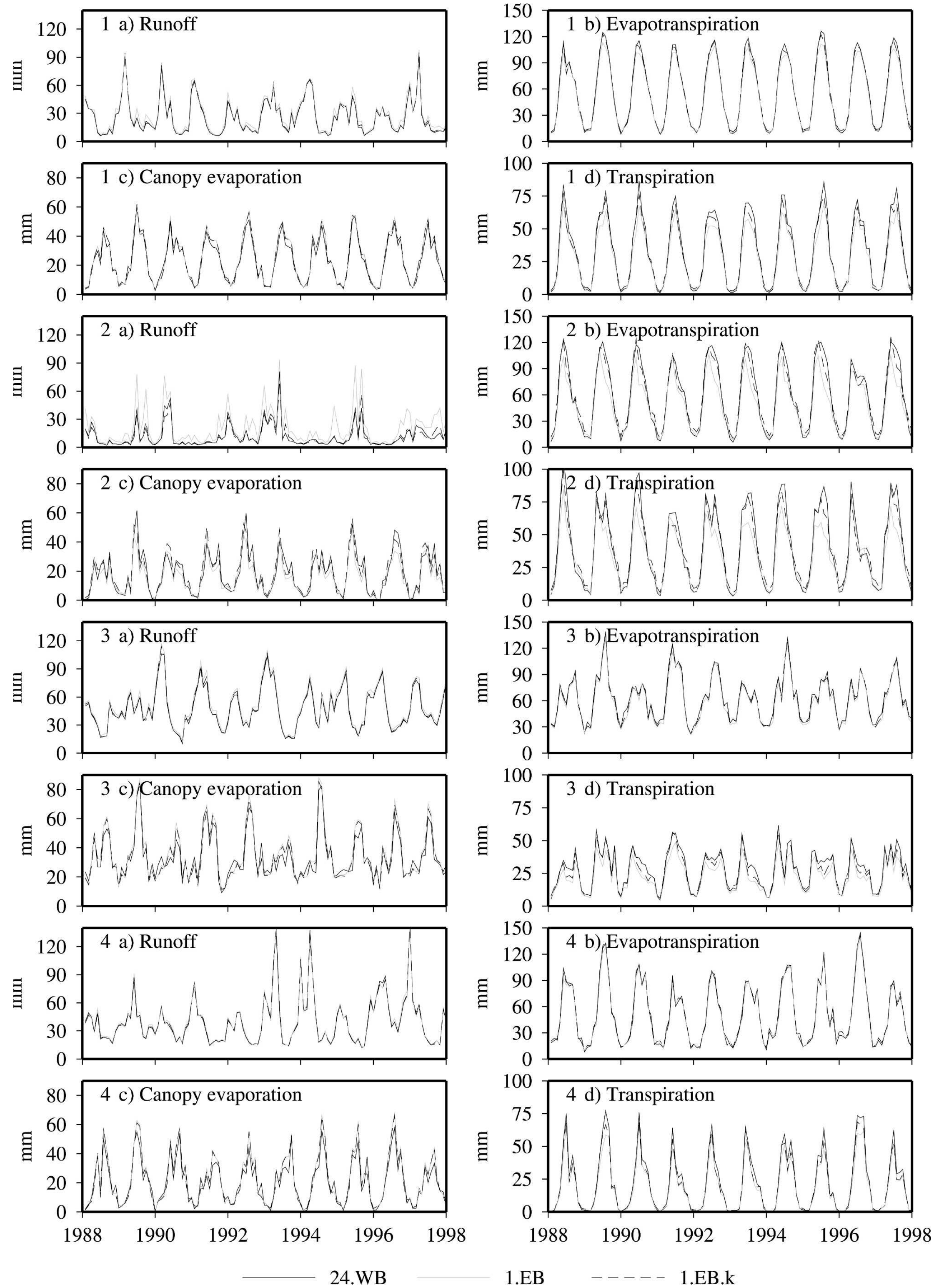

FIG. 6. Monthly values of (a) runoff, (b) evapotranspiration, (c) canopy evaporation, and (d) transpiration, at 24.WB, 3.EB, and 3.EB.k for transects 1–4.

Unauthenticated | Downloaded 04/30/21 12:30 PM UTC

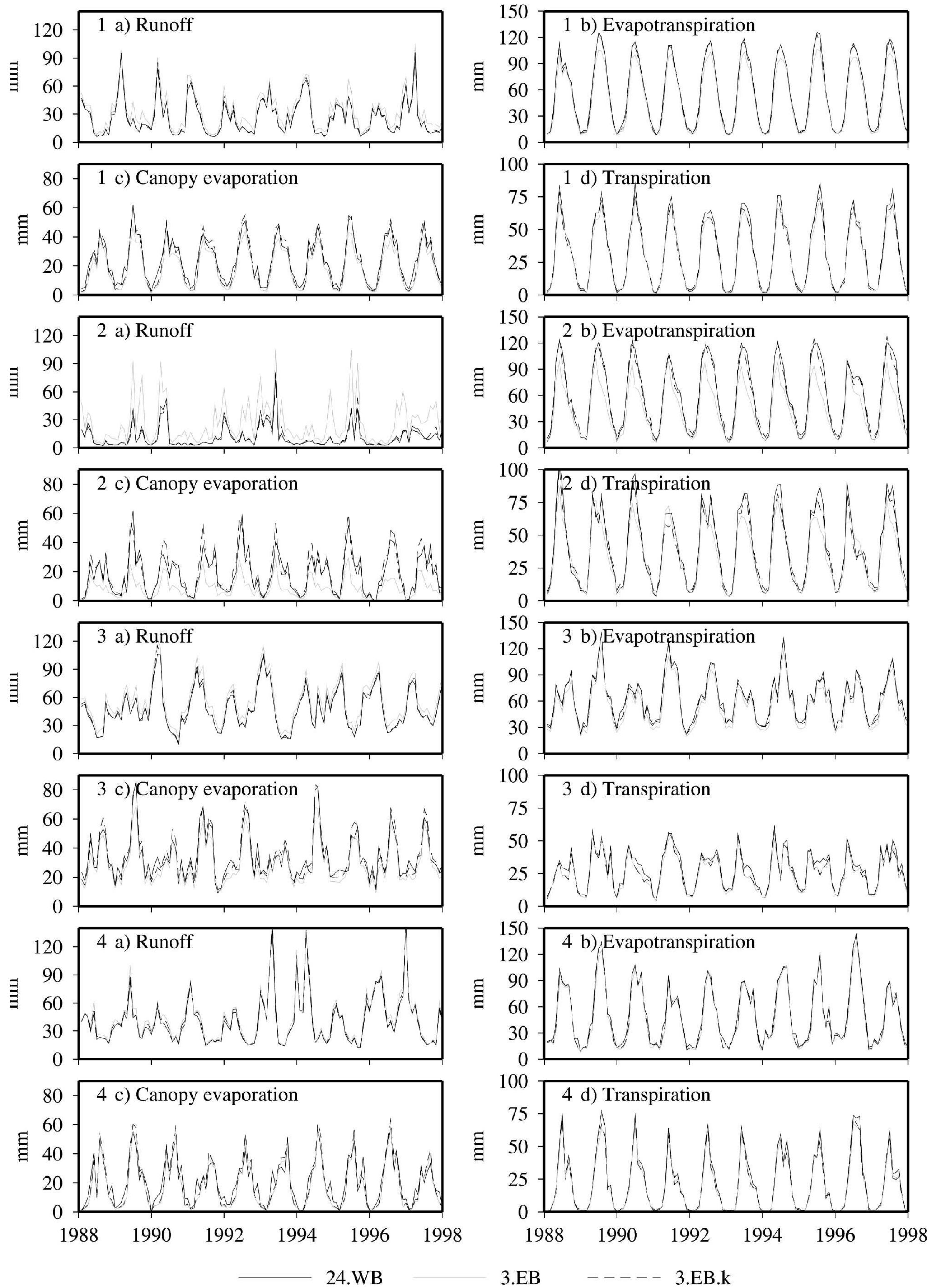

FIG. 7. Monthly values of (a) runoff, (b) evapotranspiration, (c) canopy evaporation, and (d) transpiration, at 24.WB, 1.EB, and 1.EB.k for transects 1–4.

Unauthenticated | Downloaded 04/30/21 12:30 PM UTC

where EC is canopy evaporation and TV is vegetation transpiration. SCEM-UA is a global optimization algorithm that searches through the parameter space to find the best parameter set for a given objective function. In this study, the SCEM-UA algorithm evolves toward the best correction factors by comparing monthly simulated canopy evaporation and transpiration values at subdaily time steps (3.EB and 1.EB) to the simulation results at daily time steps.

The first 5 yr of data record (1988–92) were used to estimate the correction factors. The correction factors were thereafter transferred to the remaining cells by simple interpolation, and the transects were rerun in hourly and 3-hourly energy balance mode for the entire 10-yr simulation period. Mean annual moisture fluxes for each cell at subdaily time steps compared to the fluxes at daily time steps, are shown in Fig. 5, while time series of monthly moisture fluxes for the four transects are shown in Figs. 6 and 7. The figures clearly show that the corrected runs (3.EB.k and 1.EB.k) closely match the daily water balance runs, even for the transect at 98°W, which originally had the largest runoff discrepancies.

The Nash–Sutcliffe efficiency criterion (Nash and Sutcliffe 1970) is defined as

$$\text{Efficiency} = 1 - \frac{\sum (Q_s - Q_b)^2}{\sum (Q_b - \overline{Q_b})^2}, \tag{5}$$

where Q_s represents simulated runoff values at subdaily time steps, and Q_b represents the baseline analysis (daily time steps). An efficiency value of 1 indicates a perfect fit. The Nash–Sutcliffe efficiency criterion was calculated for each transect based on monthly runoff values. For the calibration period (1988–92), the efficiencies increased substantially (see Table 2), which also shows that the efficiencies increased for the validation period (1993–97). The objective function [Eq. (4)] is based on canopy evaporation and transpiration differences. Optimizing based on runoff differences gave even better results (not shown) when considering runoff alone, but Eq. (4) was favored since the overall results (i.e., evaporation, transpiration, and soil moisture in addition to runoff) were preferable using that formulation.

TABLE 2. Nash–Sutcliffe efficiency criteria for each transect for A, the calibration period (1988–92), and B, the validation period (1993–97).

	Transect number							
	1 (37°N)		2 (98°W)		3 (40°N)		4 (33°N)	
Analysis	A	B	A	B	A	B	A	B
3.EB − 24.WB	0.81	0.79	−1.66	−1.65	0.87	0.97	0.83	0.87
3.EB.k − 24.WB	0.99	0.99	0.97	0.94	0.97	0.99	0.99	0.99
1.EB − 24.WB	0.96	0.95	−0.11	−0.22	0.98	0.98	0.95	0.97
1.EB.k − 24.WB	0.99	0.99	0.95	0.91	0.99	0.99	0.99	0.99

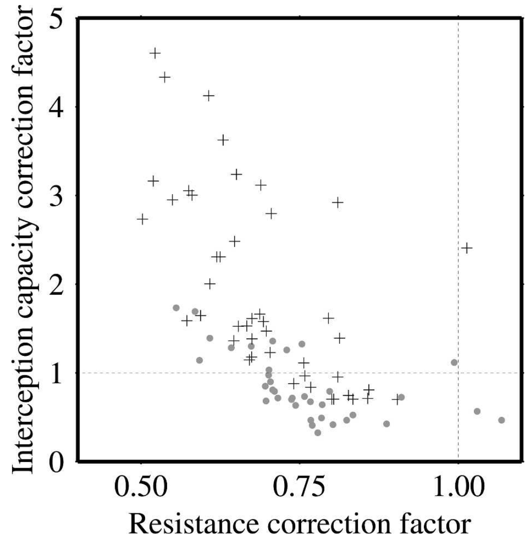

FIG. 8. Interception capacity correction factors plotted against resistance correction factors for the 46 transect cells where the search procedure was implemented (black crosses: 3.EB.k; gray dots: 1.EB.k).

The estimated interception capacity correction factors at 3.EB.k varied between 0.7 and 4.6, and the resistance correction factors varied from 0.5 to slightly above 1 (see Fig. 8). The resistance correction factors at 1.EB.k are comparable to the ones at 3.EB.k, while the somewhat higher canopy evaporation values at 1.EB compared to 24.WB results in interception correction factors below 1 for most cells except the ones at transect 2 (98°W). Figure 8, which shows interception capacity correction factors plotted against resistance correction factors, indicates that the higher the interception capacity factor, the more the resistance is corrected. The cells where the estimated interception capacity correction factor is below 1 are all dominated by overstory vegetation, typically broadleaf deciduous trees with high summer leaf area index (LAI) values. The LAI values are, however, not the only factor influencing the correction factors, as climate plays a role as well.

All model simulations in this study were performed offline (i.e., no coupling to the atmosphere, as would be the case in a coupled land–atmosphere implementation). Liu et al. (2005) have shown that calibration of a land surface model in coupled mode may result in somewhat different parameter values than those obtained in uncoupled mode. Hence, the initial parameter

Unauthenticated | Downloaded 04/30/21 12:30 PM UTC

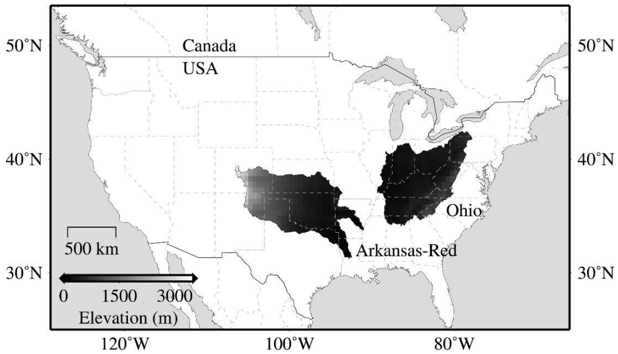

FIG. 9. Location of study basins.

values presented in this study might be sensitive to the coupled hydrologic–atmosphere environment, but this would not change the general results of the analyses presented in this paper.

5. Arkansas–Red and Ohio River basin applications

The largest differences in simulated moisture fluxes are observed between the daily water balance mode and the 3-hourly energy balance mode. The correction scheme described in the previous section was therefore tested on the 3-hourly energy balance model setup, using daily water balance simulations as the baseline run, on the Arkansas–Red and Ohio River basins (Fig. 9), to see if reasonable results can be obtained using the method for large river basins. The same calibration and validation periods as for the transects were used (1988–92 and 1993–97, respectively), and correction factors were calculated for every eighth cell, that is, one grid cell per degree latitude and longitude. The adjustment factors estimated for these "index" grid cells were then interpolated to the entire domain of 1/8° grid cells. Over the entire domain, direct estimates of the adjust-

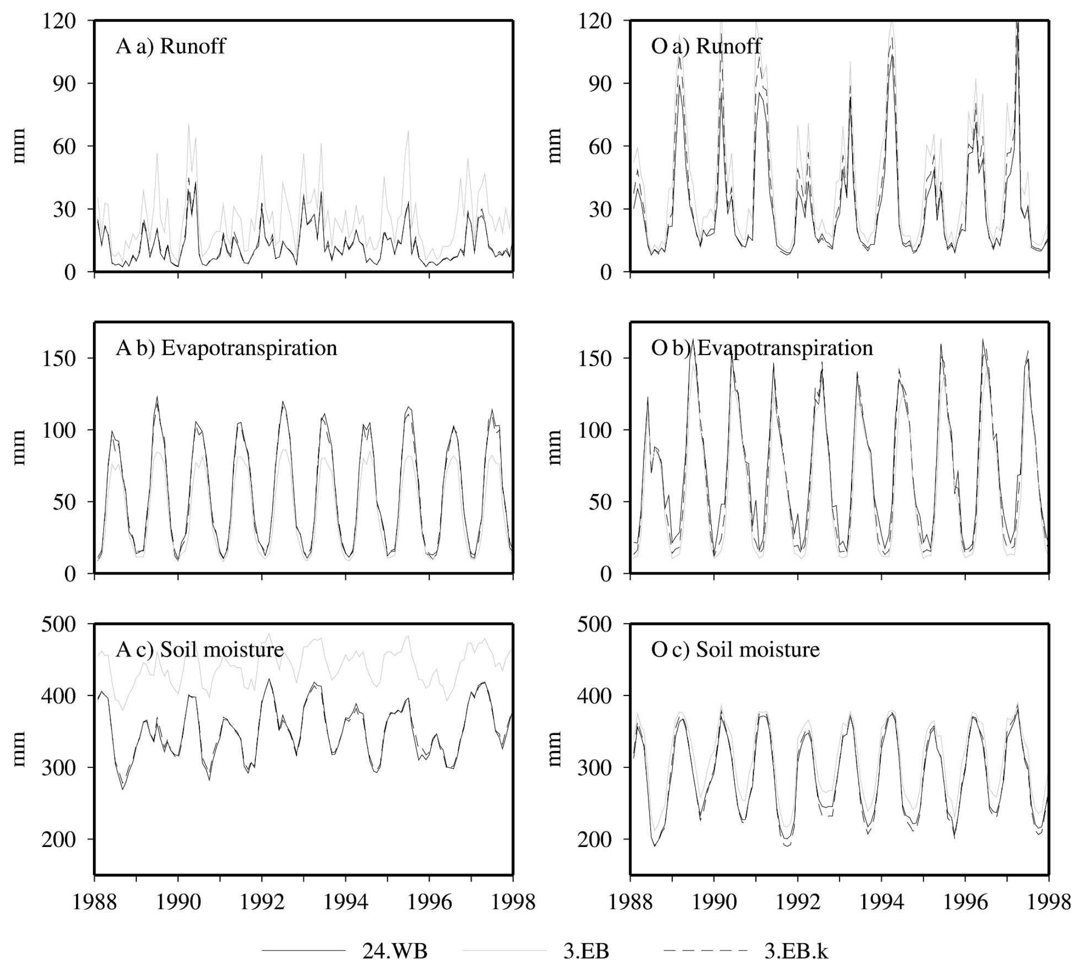

FIG. 10. Monthly values of (a) runoff, (b) evapotranspiration, and (c) soil moisture at 24.WB, 3.EB, and 3.EB.k in the Arkansas–Red (A) and Ohio River (O) basins.

Unauthenticated | Downloaded 04/30/21 12:30 PM UTC

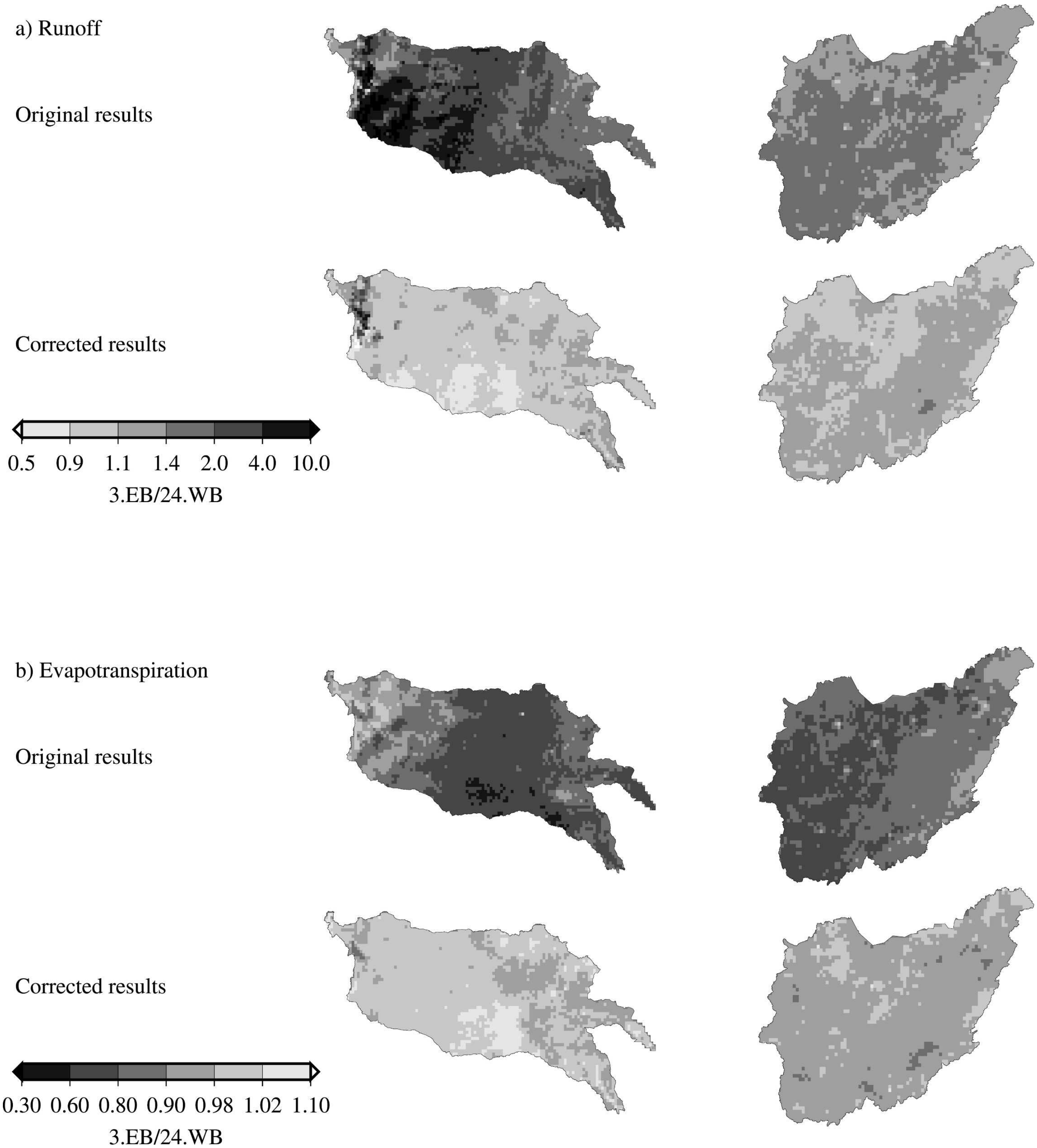

FIG. 11. Original and corrected results of mean annual runoff and evapotranspiration at 3.EB compared with the results at 24.WB, in the Arkansas–Red and Ohio River basins. Note the uneven legend intervals.

ment factors were produced for 1 in every 64 1/8° grid cells, and were interpolated to the remainder.

Figure 10 shows resulting monthly time series of simulated moisture fluxes at 24.WB, 3.EB, and 3.EB.k (3.EB.k results from the use of correction factors). Figure 11 compares runoff and evapotranspiration over the two basins. The figures show that after implementing the correction factors to 3.EB, the simulated moisture fluxes in the Arkansas–Red River basin closely match those simulated in 24.WB. The simulation results for the Ohio River basin are closer to the 24.WB results as well, but the peak streamflow values are still higher

Unauthenticated | Downloaded 04/30/21 12:30 PM UTC

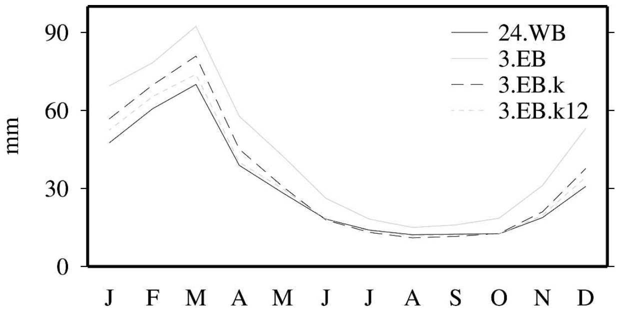

FIG. 12. Mean monthly runoff in the Ohio River basin at 24.WB, 3.EB, 3.EB.k (corrected results), and 3.EB.k12 (corrected results using monthly interception capacity correction factors).

than the 24.WB simulations. The Nash–Sutcliffe efficiency criterion, calculated based on monthly runoff values for the corrected energy balance runs for the entire 10-yr simulation period, is 0.97 and 0.91 for the Arkansas–Red and Ohio River basin, respectively.

Simulated canopy evaporation values in the Ohio River basin in energy balance mode are higher than in water balance mode during the summer, and lower during the winter. This is caused by the variation in LAI values over the year in the Ohio River basin, where large areas are dominated by broadleaf deciduous vegetation. For low LAI values, 3-hourly time steps result in lower canopy evaporation than daily time steps. However, the difference decreases as LAI increases, and when LAI is high (specific value depending on local climate) canopy evaporation at 3-hourly time steps ends up being higher than at daily time steps. Hence, canopy evaporation within a grid cell can be lower at 3-hourly time steps than at daily time steps in early spring, but higher later in the summer. This makes it difficult for the parameter estimation search to find one interception capacity correction factor that is valid throughout the year.

Based on the findings for the Ohio River basin, a slightly different correction scheme was tested. The SCEM-UA algorithm (Vrugt et al. 2003) was used to search for monthly interception capacity correction factors; that is, the canopy interception capacity was allowed to vary throughout the year. As Fig. 12 shows, this results in 3.EB results (3.EB.k12) somewhat closer to the 24.WB results in comparison with using only one interception capacity correction factor. The Nash–Sutcliffe efficiency criterion is now 0.97, compared to 0.91 using the original correction scheme.

6. North American land data assimilation system (NLDAS) reconciliation

For the NLDAS project (Mitchell et al. 2004), two somewhat different VIC modeling simulations were performed. Maurer et al. (2002) performed a 50-yr retrospective run at 3-h time steps using precipitation data from National Oceanic and Atmospheric Administration (NOAA) Co-op stations, scaled to match the long-term average of the Parameter-elevation Regressions on Independent Slopes Model precipitation climatology (Daly et al. 1994, 1997). Daily precipitation values were uniformly distributed to 3-h periods within each day, and no variability in subgrid precipitation was assumed. The results presented in Lohmann et al. (2004) are based on a 3-yr run using 1-hourly time steps, and temporally and spatially disaggregated [the latter using the algorithm of Liang et al. (1996)] precipitation. The model results presented by Lohmann et al. (2004) are driven by precipitation data from gauge-based precipitation analysis and satellite retrieval [see Cosgrove et al. (2003) for details]. The same model parameters (soil and vegetation characteristics) were used for both model setups, and both were run in energy balance mode. When comparing moisture fluxes, it is apparent

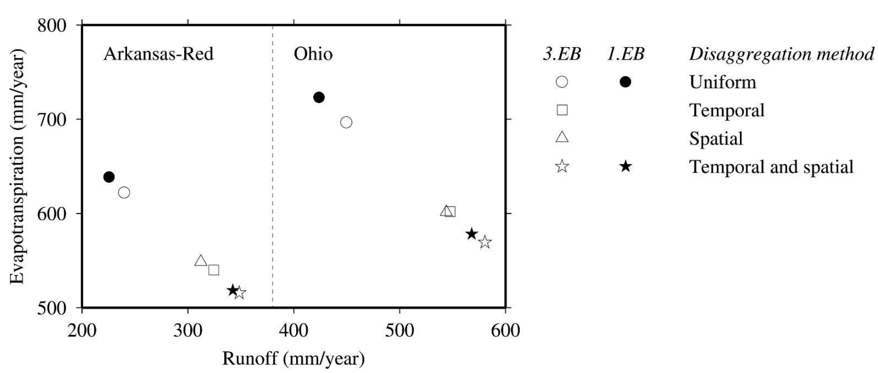

FIG. 13. Effects of time step and method of precipitation disaggregation on mean annual runoff and evapotranspiration values in the Arkansas–Red and Ohio River basins.

Unauthenticated | Downloaded 04/30/21 12:30 PM UTC

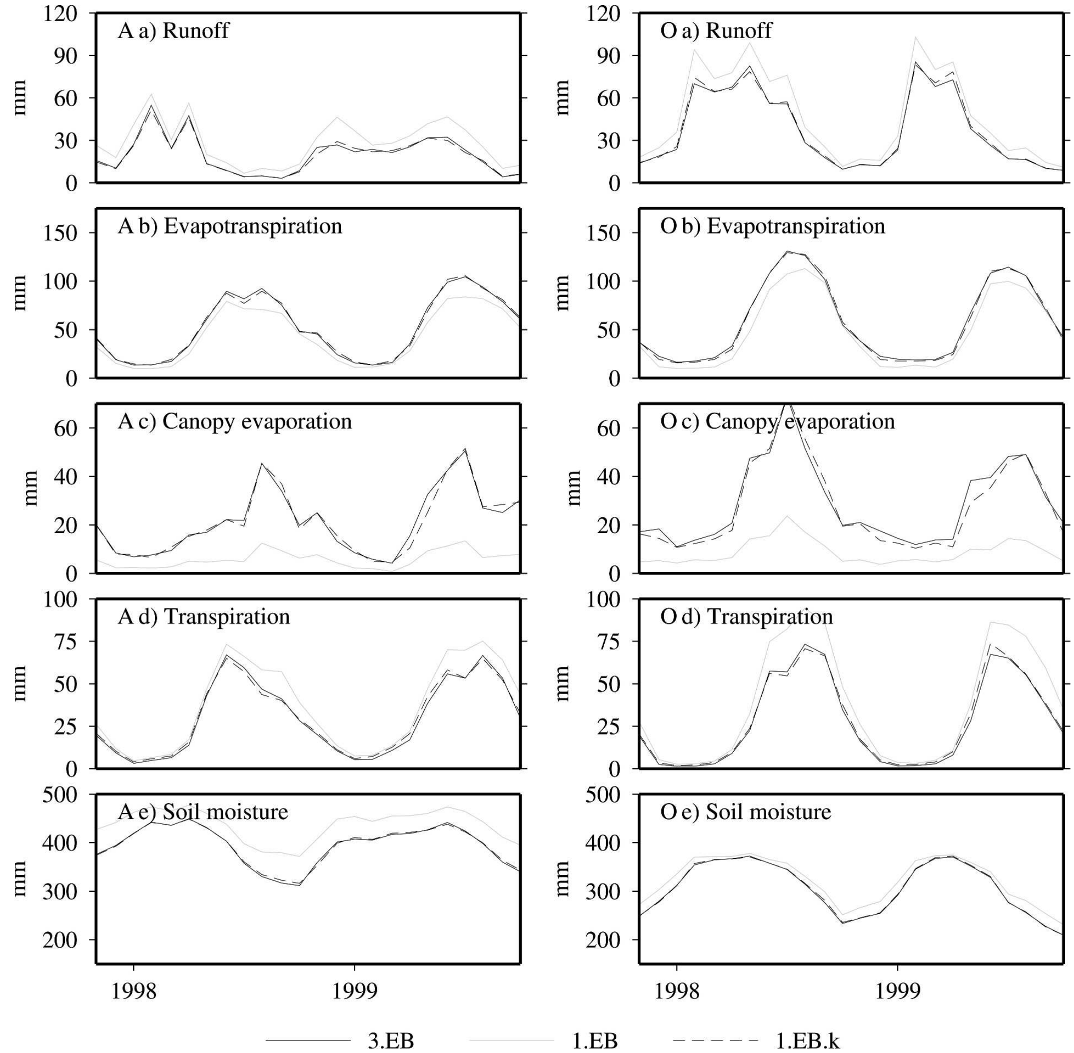

FIG. 14. Monthly values of (a) runoff, (b) evapotranspiration, (c) canopy evaporation, (d) transpiration, and (e) soil moisture at 3.EB, 1.EB, and 1.EB.k in the Arkansas–Red (A) and Ohio (O) River basins. The hourly simulations are performed using spatially and temporally disaggregated precipitation.

that the VIC results reported in Lohmann et al. (2004) have higher runoff values than reported in Maurer et al. (2002).

In order to determine how much of the difference between Maurer et al. (2002) and Lohmann et al. (2004) is due to precipitation disaggregation, and how much is due to time step, various model simulations combining different model time steps and methods of precipitation disaggregation were performed. Initial analyses showed that the surface forcings used in Lohmann et al. (2004) (incoming longwave and shortwave radiation, air pressure, vapor pressure, wind speed, and air temperature) did not influence the simulated moisture fluxes considerably, compared to using the temperature and wind data of Maurer et al. (2002). Therefore, the temperature and wind data of Maurer et al. (2002) were used in all simulations presented here. Furthermore, to remove the effects of having somewhat different precipitation amounts, the Lohmann et al. (2004) precipitation values were adjusted so that monthly totals match those used by Maurer et al. (2002).

Figure 13 shows a suite of model results for the Arkansas–Red and Ohio River basins. The sensitivity analyses are performed using various model setups for the period October 1997–September 1999 (after 1-yr spinup), that is, the same time period as presented in Lohmann et al. (2004). The results are consistent with Lohmann et al. (2004), namely, the interdependence of model setup and parameter choice and the lack of pa-

Unauthenticated | Downloaded 04/30/21 12:30 PM UTC

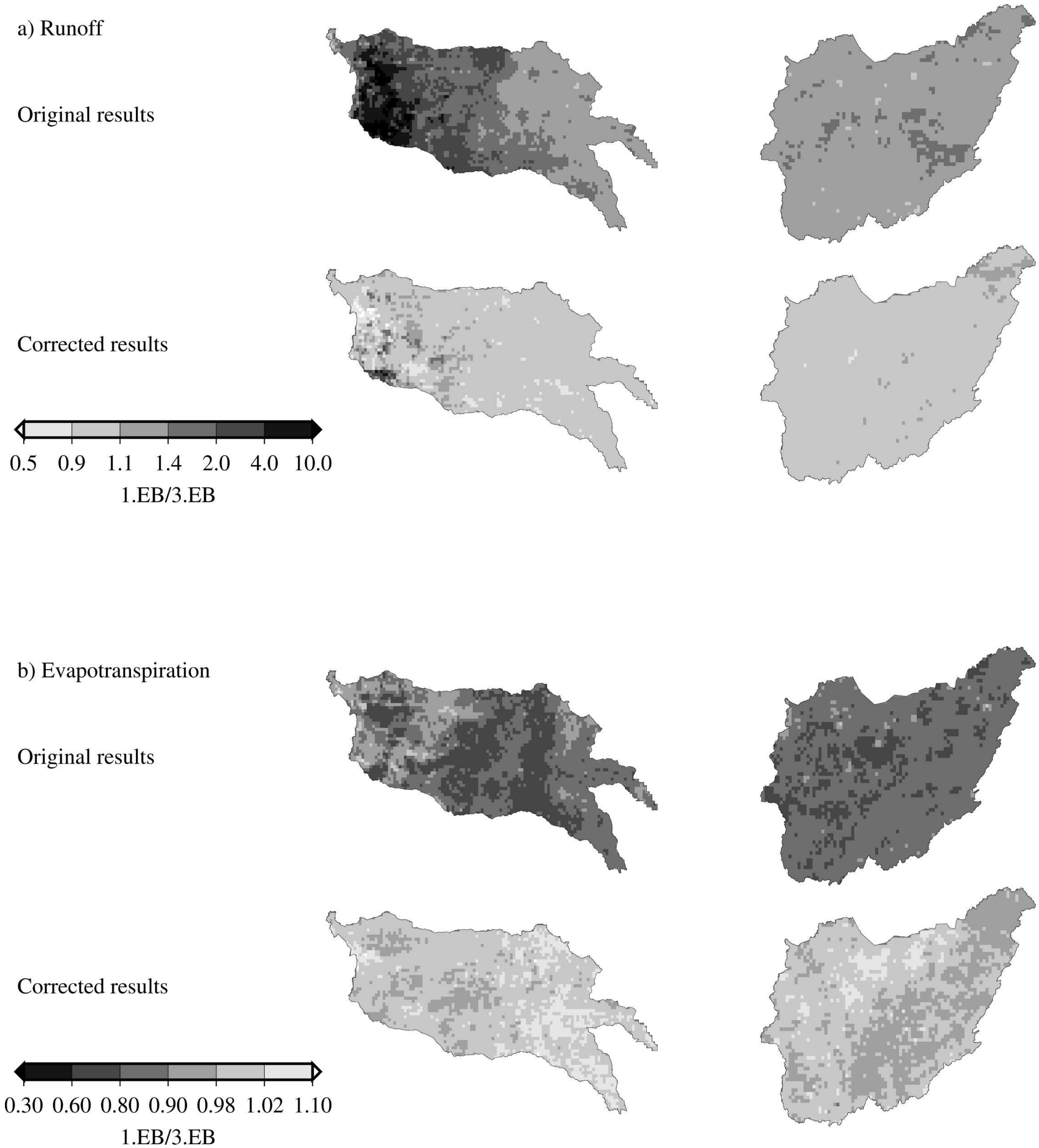

FIG. 15. Original and corrected results of mean annual runoff and evapotranspiration at 1.EB, using spatially and temporally disaggregated precipitation compared with the results at 3.EB, in the Arkansas–Red and Ohio River basins. Note the uneven legend intervals.

rameter robustness. Figure 13 indicates that the main reason for the higher runoff values at 1.EB [equivalent to the Lohmann et al. (2004) model setup] than at 3.EB [equivalent to the Maurer et al. (2002) model setup] is the method of precipitation disaggregation, and that spatial disaggregation of precipitation influences the resulting runoff values slightly less than does temporal disaggregation of precipitation. Simulated mean annual runoff at 1.EB (using temporally and spatially disaggregated precipitation) is 43% and 26% higher than at

Unauthenticated | Downloaded 04/30/21 12:30 PM UTC

3.EB (no spatially or temporally disaggregated precipitation) for the Arkansas–Red and Ohio River basins, respectively. When running the model at hourly time steps without spatially or temporally disaggregated precipitation, the resulting runoff is much more similar to the results at 3.EB. Hence, the time step difference does not appear to influence the results as much as the method of precipitation disaggregation does. This result is consistent with the results obtained when running the model with spatially and temporally disaggregated precipitation at 1- and 3-hourly time steps (for the latter the 1-h temporally disaggregated precipitation values are aggregated to 3-h time steps) (see Fig. 13).

The correction scheme presented above was used to match the hourly runs of Lohmann et al. (2004) to the 3-hourly runs of Maurer et al. (2002) for the period October 1997–September 1999 (after 1-yr spinup), that is, the same time period as presented in Lohmann et al. (2004). Monthly time series of moisture fluxes averaged over the basins are presented in Fig. 14, while Fig. 15 shows mean annual results spatially over the basins. The figures show that when using the correction scheme, the simulation results of Maurer et al. (2002) (3-hourly energy balance, no spatial or temporal disaggregation of precipitation) can successfully be matched at 1-hourly time steps using both spatially and temporally disaggregated precipitation.

7. Conclusions

Moisture fluxes simulated by the VIC model are sensitive to the time step used, to the assumptions made regarding closure of the surface energy budget, and to the method of temporal and spatial disaggregation of precipitation. Simulated canopy evaporation differences are the main reason for the discrepancies between simulated model results. In addition, factors controlling transpiration are impacted by the time step used, and by the method used to define surface temperatures (i.e., assuming surface temperature equals air temperature when running the model in water balance mode, as opposed to estimating the surface temperature when running the model in energy balance mode).

Substantial differences in resulting moisture fluxes can be seen when comparing daily water balance results with subdaily energy balance results. The difference between 3-hourly energy balance results and 1-hourly energy balance results are less significant, given that time step is the only difference between the two model setups. However, temporal and spatial disaggregation of precipitation influence resulting moisture fluxes significantly. Sensitivity analyses performed at subdaily time steps (3 and 1 h) indicate that temporal disaggregation of precipitation is the most significant factor controlling canopy evaporation at subdaily time steps, and hence transpiration and runoff as well.

The correction scheme developed shows that simulation results at different model setups can be reconciled to a large extent by introducing correction factors that adjust the canopy interception capacity and canopy resistance. In areas having relatively small differences in LAI over the year, satisfactory results can be obtained when using a constant canopy interception correction factor over the year. In areas having large interannual variations in LAI (e.g., decidous forest) the best results are obtained when allowing for interannual variation in the interception capacity correction factor. The results presented show that it is possible to calibrate the model in the computationally efficient daily water balance mode and thereafter introduce correction factors to the subdaily energy balance simulations without having to recalibrate the model.

REFERENCES

Boone, A., and Coauthors, 2004: The Rhone-Aggregation Land Surface Scheme Intercomparison Project: An overview. *J. Climate,* **17,** 187–208.

Bras, R. L., 1990: *Hydrology: An Introduction to Hydrologic Science.* Addison-Wesley, 643 pp.

Cosgrove, B. A., and Coauthors, 2003: Real-time and retrospective forcing in the North American Land Data Assimilation System (NLDAS) project. *J. Geophys. Res.,* **108,** 8842, doi:10.1029/2002JD003118.

Daly, C., R. P. Neilson, and D. L. Phillips, 1994: A statistical–topographic model for mapping climatological precipitation over mountainous terrain. *J. Appl. Meteor.,* **33,** 140–158.

——, G. H. Taylor, and W. P. Gibson, 1997: The PRISM approach to mapping precipitation and temperature. Preprints, *10th Conf. on Applied Climatology*, Reno, NV, Amer. Meteor. Soc., 10–12.

Haddeland, I., B. V. Matheussen, and D. P. Lettenmaier, 2002: Influence of spatial resolution in a macroscale hydrologic model. *Water Resour. Res.,* **38,** 1124, doi:10.1029/2001WR000854.

Holman-Dodds, J. K., A. A. Bradley, and P. L. Sturdevant-Rees, 1999: Effect of temporal sampling of precipitation on hydrologic model calibration. *J. Geophys. Res.,* **104** (D16), 19 645–19 654.

Kimball, J. S., S. W. Running, and R. Nemani, 1997: An improved method for estimating surface humidity from daily minimum temperature. *Agric. For. Meteor.,* **85,** 87–98.

Liang, X., D. P. Lettenmaier, E. F. Wood, and S. J. Burges, 1994: A simple hydrologically based model of land surface water and energy fluxes for general circulation models. *J. Geophys. Res.,* **99** (D7), 14 415–14 428.

——, ——, and ——, 1996: One-dimensional statistical dynamic representation of subgrid spatial variability of precipitation in the two-layer variable infiltration capacity model. *J. Geophys. Res.,* **101** (D16), 21 403–21 422.

Liu, Y., H. V. Gupta, S. Sorooshian, L. A. Bastidas, and W. J. Shuttleworth, 2005: Constraining land surface and atmo-

Unauthenticated | Downloaded 04/30/21 12:30 PM UTC

spheric parameters of a locally coupled model using observational data. *J. Hydrometeor.,* **6,** 156–172.

Lohmann, D., E. Raschke, B. Nijssen, and D. P. Lettenmaier, 1998: Regional scale hydrology: I. Formulation of the VIC-2L model coupled to a routing model. *Hydrol. Sci. J.,* **43,** 131–141.

——, and Coauthors, 2004: Streamflow and water balance intercomparisons of four land surface models in the North American Land Data Assimilation System project. *J. Geophys. Res.*, **109,** D07S91, doi:10.1029/2003JD003517.

Maurer, E. P., A. W. Wood, J. C. Adam, D. P. Lettenmaier, and B. Nijssen, 2002: A long-term hydrologically based data set of land surface fluxes and states for the conterminous United States. *J. Climate,* **15,** 3237–3251.

Mitchell, K. E., and Coauthors, 2004: The multi-institution North American Land Data Assimilation System (NLDAS): Utilizing multiple GCIP products and partners in a continental distributed hydrological modeling system. *J. Geophys. Res.*, **109,** D07S90, doi:10.1029/2003JD003823.

Nash, J. E., and J. V. Sutcliffe, 1970: River flow forecasting through conceptual models, 1, A discussion of principles. *J. Hydrol.,* **10,** 282–290.

Nijssen, B., R. Schnur, and D. P. Lettenmaier, 2001: Global retrospective estimation of soil moisture using the Variable Infiltration Capacity land surface model, 1980–93. *J. Climate,* **14,** 1790–1808.

——, and Coauthors, 2003: Simulation of high latitude hydrological processes in the Torne-Kalix basin: PILPS phase 2(e). 2: Comparison of model results with observations. *Global Planet. Change,* **38,** 31–53.

Schaake, J. C., V. I. Koren, Q. Duan, K. Mitchell, and F. Chen, 1996: Simple water balance model for estimating runoff at different spatial and temporal scales. *J. Geophys. Res.,* **101** (D3), 7461–7476.

Shuttleworth, W. J., 1993: Evaporation. *Handbook of Hydrology*, D. R. Maidment, Ed., McGraw Hill, 4.2–4.18.

Storck, P., 2000: Trees, snow and flooding: An investigation of forest canopy effects on snow accumulation and melt at the plot and watershed scales in the Pacific Northwest. Water Resources Series Tech. Rep. 161, Department of Civil and Environmental Engineering, University of Washington, Seattle, WA, 176 pp.

Thornton, P. E., and S. W. Running, 1999: An improved algorithm for estimating incident daily solar radiation from measurements of temperature, humidity, and precipitation. *Agric. For. Meteor.,* **93,** 211–228.

Vérant, S., K. Laval, J. Polcher, and M. De Castro, 2004: Sensitivity of the continental hydrological cycle to the spatial resolution over the Iberian Peninsula. *J. Hydrometeor.,* **5,** 267–285.

Vrugt, J. A., H. V. Gupta, W. Bouten, and S. Sorooshian, 2003: A shuffled complex evolution metropolis algorithm for optimization and uncertainty assessment of hydrologic model parameters. *Water Resour. Res.,* **39,** 1201, doi:10.1029/2002WR001642.

Wigmosta, M. S., L. W. Vail, and D. P. Lettenmaier, 1994: A distributed-hydrology-vegetation model for complex terrain. *Water Resour. Res.,* **30,** 1665–1679.

Wood, E. F., D. P. Lettenmaier, and V. G. Zartarian, 1992: A land-surface hydrology parameterization with subgrid variability for general circulation models. *J. Geophys. Res.,* **97** (D3), 2717–2728.

——, and Coauthors, 1998: The Project for Intercomparison of Land-surface Parameterization Schemes (PILPS) phase 2(c) Red–Arkansas River basin experiment: 1. Experiment description and summary intercomparisons. *Global Planet. Change,* **19,** 115–135.

Zhao, R. J., Y. L. Zhang, L. R. Fang, X. R. Liu, and Q. S. Zhang, 1980: The Xinanjiang model. *Hydrological Forecasting Proc.: Oxford Symp.*, Vol. 129, Oxford, United Kingdom, IASH, 351–356.

Unauthenticated | Downloaded 04/30/21 12:30 PM UTC